Collaboration Pursuing Method for MDO Problems

Dapeng Wang*, G. Gary Wang† and Greg F. Naterer‡

Multidisciplinary Design Optimization (MDO) problems are dominated by couplings among subsystems formulated from different disciplines. Effective and efficient collaboration between subsystems is always desirable when solving MDO problems. This work proposes a new sampling-based methodology, named the Collaboration Pursuing Method (CPM), for MDO problems. In the CPM, a new collaboration model, reflecting both physical and mathematical characteristics of couplings in MDO problems, is formulated to guide the search of feasible design solutions. The interdisciplinary consistency among coupled state parameters in MDO problems is reflected and maintained by the collaboration model. An adaptive sampling strategy is also developed to speed up the search of local optimal solutions. The new method is implemented using MATLAB® 6.0 and successfully applied to four test problems including an engineering design application.

Nomenclature

D = discrepancy of state parameters,

f = system objective function

$\mathbf{G}$ = vector of functions associated with constraints

$\boldsymbol{g}$ = vector of constraints

L = difference between the ranking numbers of the largest and smallest feasible sample points

n = number of state parameters

r = the ratio between the numbers of feasible and infeasible sample points

* Ph.D. AIAA Member, Department of Mechanical and Manufacturing Engineering, 75A Chancellors Circle, Winnipeg, Manitoba, Canada, R3T 5V6, E-mail: DapengWang@yahoo.com.
† Associate Professor. AIAA Member, Department of Mechanical and Manufacturing Engineering, 75A Chancellors Circle, Winnipeg, Manitoba, Canada. R3T 5V6, E-mail: gary_wang@umanitoba.ca.
‡ Professor. AIAA Member, Professor and Director of Research, Graduate Studies and Development, Faculty of Engineering and Applied Science, University of Ontario Institute of Technology, 2000 Simcoe Street North, Oshawa, Ontario, Email: Greg.Naterer@uoit.ca.

SP = speed factor of guidance functions

$\boldsymbol{x}$ = vector of design variables ($\boldsymbol{x}_{cs} \cup \boldsymbol{x}_i\big|_{i=1,\ldots,n}$)

$\boldsymbol{x}_i$ = vector of disciplinary/local design variables of y_i

$\boldsymbol{x}_{cs}$ = vector of design variables shared by by y_i and f. $\boldsymbol{x}_{csi} \cap \boldsymbol{x}_{csj}$, $i \neq j$, does not have to be Ø

$\tilde{\boldsymbol{x}}_i$ = vector of explicit and implicit design variables of y_i

$\boldsymbol{y}$ = vector of state parameters, $\{y_1,\ldots y_n\}$

$\boldsymbol{y}_{ci}$ = vector of state parameters output from other subsystems to subsystem i, $\{y_j\}, j \neq i$

Y_i = function associated with y_i

$\bar{\mathrm{Y}}$ = implicit approximate function

$\bar{\bar{\mathrm{Y}}}$ = explicit approximate function

σ = standard deviation

I. Introduction

A large engineering problem often covers several complex and coupled physical disciplines / subsystems. For example, a helicopter air intake scoop design involves couplings among de-icing, aerodynamic performance, and engine performance.[1,2] These disciplines usually rely on computationally intensive processes for analysis, e.g., Finite Element Analysis (FEA) and Computational Fluid Dynamics (CFD). Engineering design is driven by today's increasingly competitive global market, and is confined by all aspects of design over the product life cycle, such as performance, life-cycle cost, reliability, maintainability, vulnerability, and so forth.[3] Multidisciplinary Design Optimization (MDO), or Multidisciplinary Design Synthesis, is a methodology for solving such complex and coupled engineering problems. MDO consists of a wide scope of issues including design synthesis, sensitivity analysis, approximation concepts, and optimization methods and strategies. It has been extensively reviewed in references.[4-10] This paper is dedicated to a new sampling-based methodology that does not apply sensitivity analyses when solving MDO problems.

A general MDO problem is defined by

$$\begin{aligned} &\min\ f\left(\boldsymbol{x}_{cs}, \boldsymbol{y}\right) \\ &\text{subject to: } y_i = \mathrm{Y}_i\left(\boldsymbol{x}_i, \boldsymbol{x}_{csi}, \boldsymbol{y}_{ci}\right), i = 1, ..., n \\ &\qquad \boldsymbol{g} = \mathrm{G}\left(\boldsymbol{x}, \boldsymbol{y}\right) \le 0 \end{aligned} \tag{1}$$

In Eq. (1), $\boldsymbol{y}$ is governed by

$$\begin{cases} y_1 = \mathrm{Y}_1\left(\boldsymbol{x}_1, \boldsymbol{x}_{cs1}, \boldsymbol{y}_{c1}\right) \\ ... \\ y_i = \mathrm{Y}_i\left(\boldsymbol{x}_i, \boldsymbol{x}_{csi}, \boldsymbol{y}_{ci}\right) \\ ... \\ y_n = \mathrm{Y}_n\left(\boldsymbol{x}_n, \boldsymbol{x}_{csn}, \boldsymbol{y}_{cn}\right) \end{cases} \tag{2}$$

Eq. (2) describes the System Analysis (SA) or the Multidisciplinary Analysis (MDA). The solution of Eq. (2) is normally calculated by an iterative procedure (such as the Gauss-Seidel iterative method for linear equations and the Steepest Descent method for nonlinear equations[11]), when given a set of $\boldsymbol{x}$, the initial guess of $\boldsymbol{y}$, convergence criterion determined by a specified accuracy tolerance, and maximum number of iterations. State Parameters, $\boldsymbol{y}$, usually represent some physical features, e.g., temperature, and they are often calculated by computationally intensive processes. The standard MDO formulation in Eq. (1) is also called the Multidisciplinary Feasible (MDF) method in the nonlinear programming community, or the "All-in-One" method in the engineering community.[12] It can be solved by conventional optimization algorithms, such as gradient-based methods, treating the SA/MDA as equality constraints. The main difficulty of applying "All-in-One" in practice is that the computational cost could be prohibitive since the SA/MDA is frequently called during the optimization process. From this sense, reducing the number of calls to the SA/MDA can improve the performance on an MDO method.

From the engineering perspective, decomposition strategies have been applied to formulate and solve MDO problems. Global Sensitivity Equations (GSE) are used in Linear Decomposition methods, such as Concurrent Subspace Optimization (CSSO),[13-17] and Bi-level Integrated System Synthesis (BLISS).[18,19] The Linear Decomposition methods linearize a coupled design system in the neighborhood of a feasible design. It can be imagined that the optimum solution will be reached along a piecewise path in the design variable space, and a local optimum solution could be obtained. Another decomposition-based MDO method is the Collaborative Optimization

(CO),[20-23] which utilizes slack-variables to decouple subsystems. It was found that CO has difficulties preserving the standard Karush-Kuhn-Tucker condition due to its formulation structure.[24,25] Furthermore, a converged solution is not guaranteed. This work is motivated by a novel collaboration model, which is constructed based on the expression of couplings from mathematical and physical perspectives. This collaboration model has a similar role to GSE for maintaining the interdisciplinary consistency of couplings in a sampling-based optimization process.

The proposed new methodology, named the Collaboration Pursuing Method (CPM), aims to search for the global optimum solution of an MDO problem with a short turn-around time. It maintains the consistency of couplings among state parameters by a collaboration model implemented with Radial-basis Functions (RBF). The Mode-Pursuing Sampling (MPS) method is applied as a global optimizer module in the CPM.[26,27] Section II introduces the proposed collaboration model. Sections III and IV briefly reviews the Radial-basis Function, and the MPS method, respectively. The algorithm of the CPM will be elaborated in Section V, and results of test cases are shown in Section VI.

II. Collaboration Model

MDO problems are dominated by couplings among state parameters. Effective and efficient collaboration between subsystems (i.e., interdisciplinary consistency) is always desirable when solving MDO problems. Collaboration among subsystems in Linear Decomposition methods is maintained by GSE. In CO, coupled subsystems are relaxed by issuing some slack-variables from the system level to disciplinary analyses. Then the interdisciplinary consistency is pursued in the system level by extra equality constraints, which are the match between the targets issued from the system level and their corresponding values returned from subsystems.

In a sampling process, it is not certain if any set of design variables, $\boldsymbol{x}$, can produce feasible values of its state parameters governed by Eq. (2). This section introduces a Collaboration Model to help screen out, from a sample pool, infeasible sample points and select feasible sample points subject to SA/MDA. A feasible sample point subject to SA/MDA means that the point satisfies the simultaneous equations defined in Eq. (2). A feasible sample point covers "feasibility" associated with both the physical constraints of subsystems, as well as the interdisciplinary consistency. The selected sample points subject to SA/MDA have a high probability of maintaining the consistency of coupled disciplines. Therefore the Collaboration Model can be viewed as a filter for a sampling process.

Specifically, this Collaboration Model can be elaborated by using a general two-state-parameter SA/MDA problem defined by

$$\begin{aligned} y_1 &= \mathrm{Y}_1\left(\boldsymbol{x}_1, \boldsymbol{x}_{cs1}, y_2\right) \\ y_2 &= \mathrm{Y}_2\left(\boldsymbol{x}_2, \boldsymbol{x}_{cs2}, y_1\right) \end{aligned} \tag{3}$$

In Eq. (3), y_1 is an explicit function reflecting the physical relation between y_1 and its variables, i.e., $\boldsymbol{x}_{cs1}$, $\boldsymbol{x}_1$, and y_2. Meanwhile, y_1 is an implicit function of $\boldsymbol{x}$, which is the union of $\boldsymbol{x}_1$, $\boldsymbol{x}_2$, $\boldsymbol{x}_{cs1}$ and $\boldsymbol{x}_{cs2}$. The situation is similar for y_2. Intrinsically, all state parameters, $\boldsymbol{y}$, are only implicitly affected by their associated design variables. The implicit function of state parameters uncovers mathematical dependencies between state parameters, $\boldsymbol{y}$, and design variables, $\boldsymbol{x}_{cs1}$, $\boldsymbol{x}_1$, $\boldsymbol{x}_{cs2}$, and $\boldsymbol{x}_2$.

Recall Eq. (2). The proposed Collaboration Model is constructed based on two dependent approximations of coupled state parameters. One is the approximation of the implicit function and the other is of the explicit function. This work employs a Radial-basis Function (RBF) to model the implicit and explicit approximations as follows:

$$\overline{y}_i = \overline{\mathrm{Y}}_i\left(\tilde{\boldsymbol{x}}_i\right), i = 1, ..., n \tag{4}$$

$$\overline{\overline{y}}_i = \overline{\overline{\mathrm{Y}}}_i\left(\boldsymbol{x}_i, \boldsymbol{x}_{csi}, \overline{\boldsymbol{y}}_{ci}\right), i = 1, ..., n \tag{5}$$

where, $\tilde{\boldsymbol{x}}_i$ includes all associated design variables of the state parameter y_i evaluated by the approximate implicit function. In MDO problems where all state parameters are coupled with each other (in other words, values of $\boldsymbol{y}$ are evaluated simultaneously with a SA/MDA), $\tilde{\boldsymbol{x}}_i$ is the same as $\boldsymbol{x}$ defined in Eq. (1). For example, $\tilde{\boldsymbol{x}}_i$ is the union of $\boldsymbol{x}_1$, $\boldsymbol{x}_2$, $\boldsymbol{x}_{cs1}$, and $\boldsymbol{x}_{cs2}$ in Eq. (3). In other situations where at least one state parameter is not coupled with any of other state parameters (i.e., $\boldsymbol{y}_{ci}$ is empty in the y_i function in Eq. (1)), and some or all of its design variables do not exist in other coupled state parameters' function, $\tilde{\boldsymbol{x}}_i$ is a sub-set of $\boldsymbol{x}$. In general, the dependency analysis of state parameters is necessary to determine which state parameter should be in Eq. (2) and which design variable should be considered in the Collaboration Model. The value of y_i calculated by the approximate implicit function, Eq. (4), is represented by $\overline{y}_i$, and sequentially, the approximate value of y_i marked as $\overline{\overline{y}}_i$ can be explicitly evaluated by Eq.

(5), given $\boldsymbol{x}_i$, $\boldsymbol{x}_{csi}$ and $\bar{\boldsymbol{y}}_{ci}$. For a set of given design variables $\boldsymbol{x}$, the interdisciplinary discrepancy of state parameters, D, can be determined by

$$D = \sum_{i=1}^{n} \left| \bar{y}_i - \bar{\bar{y}}_i \right| \tag{6}$$

If the value of D is small, then this set of design variables, $\boldsymbol{x}$, is possibly feasible subject to SA/MDA.

The Collaboration Model defined in Eqs. (4)-(6) gives a distribution of the interdisciplinary discrepancy subject to SA/MDA for a group of sample points. It means that sample points with a smaller value of D are more likely feasible subject to SA/MDA than those with a larger value of D. The effectiveness of the Collaboration Model is shown by applying the Collaboration Model to a problem, which is the SA/MDA process of Test Case 1 (in Section VI) defined by

$$\begin{aligned} & y_1 = x_1 + x_2 - 2 + (y_2 / 1.5)^4 \\ & y_2 = x_3 + x_4 - 2 + (y_1 / 1.8)^4 \\ & \text{subjec to: } 1 \le x_1, x_2, x_3, x_4 \le 1.9 \end{aligned} \tag{7}$$

In total, 100 random sample points generated in the design variable space, (x_1, x_2, x_3, x_4) are applied for studying the effectiveness of the proposed Collaboration Model. Five experimental points, listed in Figure 1, are randomly generated and used for the RBF approximations defined in Eqs. (4) and (5). After applying the Collaboration Model for calculating the interdisciplinary discrepancy value, D, of the 100 random samples, the distribution of D over the 100 sample points is depicted in an ascending order in terms of the value of D in Figure 1. The real feasibility of the 100 sample points subject to SA/MDA in Figure 1 is determined based on evaluations of $\boldsymbol{y}$ of the 100 points by calling the SA/MDA process. Sample points marked with 'dot' signs are feasible, and points plotted with "plus" signs are infeasible. As expected, the sample points with a small value of D in Figure 1 are more possibly feasible subject to SA/MDA than others with a large value of D. The effectiveness of the Collaboration Model was also demonstrated in Ref. 27 by implementing the above study with 500 and 1000 random sample points, respectively.

Since the Collaboration Model is built on the response surface model, i.e., Radial-basis Functions, an intensive study of the Collaboration Model was conducted in Ref. 28. In particular, the relation between the effectiveness of the Collaboration Model and the accuracy of the RBF models can be shown by testing a SA/MDA problem defined in Eq. (8):

$$\begin{aligned} y_1 &= e^{x_1} + 0.01y_2^2 \\ y_2 &= e^{x_2} + 0.01y_1^2 \end{aligned} \tag{8}$$

where $3.5 \le x_1 \le 4.5$ and $0 \le x_2 \le 1$. A fixed set of 100 random sample points are used to demonstrate the improvement of the Collaboration Model with more accurate RBF models. From the point of view of approximation modeling, the accuracy of the RBF models should be improved with more experimental points. In this paper, 2 – 6 experimental points are sequentially chosen from Table 2, respectively, for setting up the RBF models needed by the Collaboration Model. Each Collaboration Model yields a distribution of the 100 sample points' discrepancy of coupled state parameters in an ascending order in Figures 2-4. Also, the feasibility of the 100 sample points is checked by calling the SA/MDA and it is represented with dots (feasible) or plus signs (infeasible). As aforementioned, the purpose of the Collaboration Model is to separate feasible and infeasible sample points subject to SA/MDA, based on the sample points' discrepancy distribution. In Figures 2-4, the length of an overlapped segment, L, is equal to the difference between the largest ranking number of feasible sample points, and the smallest ranking number of infeasible points. L indicates the uncertain region of D values when both feasible and infeasible points are possible. The parameter, r, is the ratio between the total number of feasible and infeasible points in the overlapping segment of the length L. In general, the shorter the overlapped segment length L and the larger the ratio r imply a more effective Collaboration Model. As shown in Figures 2-4, r is increased from 1.44 based on a low accuracy RBF model to 5.125 for a more accurate RBF model, and the length of the overlapped segment of the discrepancy distribution curve is reduced from 83 to 49. From this demonstration, the effectiveness of the Collaboration Model can be improved by increasing the accuracy of the RBF models.

The Collaboration Model is constructed by two mutually dependent approximation functions, which reflect both physical characteristics and mathematical dependency of the SA/MDA. Sample points are distinguished by a feasibility distribution subject to SA/MDA in terms of their interdisciplinary discrepancy values determined by the

Collaboration Model. The Collaboration Model serves a key role in the CPM and could be a general method for other sampling-based MDO methods. More details about the Collaboration Model are documented in Refs. 27 and 28.

III. Review of the Radial-basis Function

A Radial-basis Function (RBF) can implement an $R^m \rightarrow R^1$ nonlinear mapping from the design variable space (of a state parameter y_i), $\boldsymbol{x}$, to y_i, where m is the dimensionality of design variables $\boldsymbol{x}$.[30] The nonlinear mapping becomes more accurate with more experimental points. In general, given a set of E different design variables $\left\{\boldsymbol{x}^{(e)} \in R^m, e = 1, 2, ..., E\right\}$ and a corresponding set of E real numbers $\left\{y_i^e \in R^1 \mid e = 1, ..., E\right\}$, the RBF can be expressed in the following form.

$$\tilde{y}_i(\boldsymbol{x}) = p(\boldsymbol{x}) + \sum_{e=1}^{E} \alpha_i \varphi\left(\left\|\boldsymbol{x} - \boldsymbol{x}^{(e)}\right\|\right) \tag{9}$$

where p is a linear polynomial, $\tilde{y}_i\left(\boldsymbol{x}^{(e)}\right) = y_i^e$, $\left\{\varphi\left(\left\|\boldsymbol{x} - \boldsymbol{x}^{(e)}\right\|\right), e = 1, 2, ..., E\right\}$ is a set of E functions, known as radial-basis functions. $\|\bullet\|$ denotes a norm, which is usually Euclidean; and α_i are unknown coefficients (weights) calculated by a set of simultaneous linear equations. The input data points, $\boldsymbol{x}^{(e)} \in R^m$, e = 1, 2, …, E, are used as centers of the radial-basis functions. There is a large class of radial-basis functions including the multiquadrics, inverse multiquadrics, Gaussian functions, thin-plate spline, linear Radial-basis Function, etc. For simplicity, we choose the linear Radial-basis Function in this work as follows:

$$\tilde{y}_i(\boldsymbol{x}) = \sum_{e=1}^{E} \alpha_i \left\|\boldsymbol{x} - \boldsymbol{x}^{(e)}\right\| \tag{10}$$

According to Micchelli's Theorem,[29,30] as long as $\left\{\boldsymbol{x}^{(e)}\right\}_{e=1}^{E}$ is a set of distinct points, Eq. (10) is not singular in the solution for α_i. The reason to choose the RBF is because the RBF approximation passes through all experimental

points and gives a good accuracy around the experimental points. Also, it is easy to implement. The linear Radial-basis Function is applied to Eqs. (4) and (5) for implementing the Collaboration Model. It is to be noted that, from the algorithm of the CPM, the RBF model is only used as a guide for sampling rather than a surrogate of the original function based on which optimization is performed. Also, although RBF is chosen as the approximation method in this work, neither the Collaboration Model nor CPM dictates the exclusive use of RBF for approximation.

IV. Review of Mode-Pursuing Sampling Method

The Mode-Pursuing Sampling (MPS) method is used as a global optimizer in the CPM and it is thus briefly introduced in this section. The MPS was developed as a method to search for the global optimum of a black-box function. It is a discriminative sampling method that generates more sample points around the current minimum than other areas, while statistically covering the entire search space.[31] The main procedure of the MPS can be elaborated when solving Eq. (11) (the general formulation of an optimization problem) as follows:

$$\begin{aligned} &\min\ f(\boldsymbol{x}) \\ &\text{subject to: } \boldsymbol{g}(\boldsymbol{x}) \le 0 \end{aligned} \tag{11}$$

1. Generate *ki* initial experimental points through a random sampling process in the design variable space: $\boldsymbol{x}^{(1)}$, $\boldsymbol{x}^{(2)}$, …, $\boldsymbol{x}^{(ki)}$, and evaluate their corresponding objective function values of *f*: $f(\boldsymbol{x}^{(1)})$, $f(\boldsymbol{x}^{(2)})$,…, $f(\boldsymbol{x}^{(ki)})$. The objective function, *f*, in Eq. (11) is approximated with a Radial-basis Function in Eq. (12) based on all currently available function values, i.e., $f(\boldsymbol{x}^{(1)}), f(\boldsymbol{x}^{(2)}), \ldots, f(\boldsymbol{x}^{(ki)})$.

$$\hat{f}(\boldsymbol{x}) = \sum_{e=1}^{ki} \alpha_i \left\| \boldsymbol{x} - \boldsymbol{x}^{(e)} \right\| \tag{12}$$

such that $\hat{f}\left(\boldsymbol{x}^{(e)}\right) = f\left(\boldsymbol{x}^{(e)}\right), e = 1, ..., ki.$

2. Randomly create a large number of samples, *p*, e.g., $p = 10^4$, in the design variable space, $[\boldsymbol{x}_{Lb}, \boldsymbol{x}_{Ub}]$. All sample points' approximated objective function values, $\hat{f}\left(\boldsymbol{x}_q\right)$ (q = 1, …, p), are evaluated by Eq. (12). A distribution, *GF*, as shown in Figure 5-(a), is defined by ranking *p* samples in an ascending order in terms of the value of

$\hat{f}\left(\boldsymbol{x}_q\right)$.

3. Define a Guidance Function, $\overline{GF}\left(\boldsymbol{x}_q\right)$ based on the *GF* distribution generated in Step 2 as follows:

$$\overline{GF}\left(\boldsymbol{x}_q\right) = c_0 - \hat{f}\left(\boldsymbol{x}_q\right),\ q = 1, ...,\ p \tag{13}$$

where c_0 is a constant such that $c_0 \geq \hat{f}\left(\boldsymbol{x}_q\right),\ q = 1, ...,\ p$, as shown in Figure 5-(b).

4. Cumulatively sum up $\overline{GF}\left(\boldsymbol{x}_q\right)$ over *p* sample points to build up a new function $CG(\boldsymbol{x})$ by

$$CG\left(\boldsymbol{x}_q\right) = \frac{\sum_{j=1}^{q} \overline{GF}\left(\boldsymbol{x}_j\right)}{\sum_{i=1}^{p} \overline{GF}\left(\boldsymbol{x}_i\right)},\ q = 1, ...,\ p \tag{14}$$

$CG(\boldsymbol{x})$ is plotted in Figure 5-(c). This new function is used as a guide for sampling. It reflects a certain 'bias' to a random selection from the set of $\hat{f}\left(\boldsymbol{x}_q\right)$ (q = 1, …, p) due to its upper convex shape. In other words, the probability of being selected for each sample in the space of $\hat{f}\left(\boldsymbol{x}_q\right)$ (q = 1, …, p) is not equal. Instead, sample points with a small value of $CG(\boldsymbol{x})$ have a higher probability to be selected than other points with a large value of $CG(\boldsymbol{x})$.

5. Furthermore, applying a speed factor *SP*,[§] the intensity of preference of $CG(\boldsymbol{x})$ to sample points whose value of $\hat{f}$ is small can be increased by

$$\overline{CG}\left(\boldsymbol{x}_q\right) = \left(CG\left(\boldsymbol{x}_q\right)\right)^{SP},\ 0 < SP \leq 1,\ q = 1, ...,\ p \tag{15}$$

[§] The value of *SP* is up to designers. In general, a small *SP* could result in a local optimum; a large *SP* costs more computational efforts in searching for the global optimum.

As a result, a certain number of sample points will be selected randomly by a one-to-one mapping between a series of random values generated within [0, 1] and the distribution of $\overline{CG}(\boldsymbol{x})$, as shown in Figure 5-(d). For example, a random value is given as 0.4899. Its corresponding sample ranking number is 600 in Figure 5-(d). Then the sample point with the ranking number of 600 in $\overline{CG}(\boldsymbol{x})$ is chosen as one of the new experiments. In this way, more sample points with low ranking number values are selected than those with high ranking number values for the next sampling iteration. The total number of chosen sample points is usually between three and five.[**]

6. Use all experiments including the initial experiments to form Eq. (12). Then, repeat steps 2–6 until a certain convergence criterion is satisfied.

In Ref. 31, constraints, $\boldsymbol{g}$, are considered to be inexpensive functions of design variables, $\boldsymbol{x}$. Therefore, sample points violating $\boldsymbol{g}$ are discarded in the random sampling process in step 2 before approximating f. This situation, however, rarely happens in MDO problems since $\boldsymbol{g}$ involves state parameters, which are usually evaluated by computationally expensive processes. In each iteration, most new experiments are selected from sample points where a small value of $\hat{f}$ exists. Meanwhile, sample points are also chosen from other potential areas, even though these points have a large value of $\hat{f}$. MPS is thus, in essence, a discriminative sampling method. Compared with other optimization methods applying approximation techniques, MPS retains the possibility to pursue the optimum solution, not only along the direction with a high gradient value, but also statistically in other potential directions. It was proved that MPS converges to the global optimum of $f(\boldsymbol{x})$, as long as $f(\boldsymbol{x})$ is continuous in the neighborhood of the global optimum.[31] Based on the idea of building a guidance function, MPS can be customized and applied to other problems, such as multi-objective optimization.[32] In the next section, the framework of the Collaboration Pursuing Method will be explained.

V. Collaboration Pursuing Method

The Collaboration Pursing Method (CPM) is a sampling-based method. The basic idea of the CPM is to select some sample candidates from a sample pool for optimization. These selected sample points are preferred to be

[**] The number of new experiments depends on designers. The more experiments chosen, the more computational cost required.

feasible subject to SA/MDA and the constraints. The Collaboration Model introduced in Section II is applied for choosing feasible sample points subject to SA/MDA. Iteratively, CPM selects some sample candidates from a sample pool to search for the global optimum solution. The architecture of the CPM is shown in Figure 6. The global optimum solution is achieved with the MPS method in the CPM. Since the effectiveness and efficiency of sampling-based methods are related to the number of design variables as well as the range of design variables, an Adaptive Sampling process is applied within the neighborhood of the current best solution, $\boldsymbol{x}^*$, which is similar to a trust region.[33] Similar work has been done in Ref. 34, while the Adaptive Sampling in this work is much simpler.

The detailed process of the CPM is illustrated in Figure 7 and elaborated as follows:

(1) *Initialization* – steps 1 and 2: The CPM starts with several initial feasible experimental points (subject to both SA/MDA and the constraints), e.g., 4, by calling the SA/MDA process. This procedure is based on a random sampling process in the design variable space. Initial experiments, or sample points, will be saved in the database of experiments.

(2) In each CPM iteration, several sample candidates are selected from a large sample pool for optimization. From the 1st CPM iteration on, two sampling processes take place in the beginning of each CPM iteration.

   a) *Global Sampling* – step 3: A random sampling process employed in the original design space, $[\boldsymbol{x}_{Lb}, \boldsymbol{x}_{Ub}]$, is called Global Sampling. The Global Sampling generates p random sample points, e.g., 10^4, which will be processed by MPS to search for the global optimum solution.

   b) *Adaptive Sampling* – step 4: A random sampling process for generating p_3 random sample points in the neighborhood of the current best solution, $\boldsymbol{x}^*$, is called Adaptive Sampling. The idea of the Adaptive Sampling is to have more sample points in a small region around the current best solution. If the Adaptive Sampling still cannot improve the objective function value with a certain number of random sample points, the size of the small region should be decreased to increase the effectiveness of the Adaptive Sampling. The center of the small region will be continually updated until the optimization process reaches a local optimum, as shown in Figure 8. The Adaptive Sampling searches for local optimum solutions and speeds up the optimization process. The range of design variables for Adaptive Sampling is determined by

$$\left[\left(\boldsymbol{x}^* - \Delta\left(\boldsymbol{x}_{Ub} - \boldsymbol{x}_{Lb}\right)\right), \left(\boldsymbol{x}^* + \Delta\left(\boldsymbol{x}_{Ub} - \boldsymbol{x}_{Lb}\right)\right)\right] \tag{16}$$

where Δ is a preset ratio between 5% and 30% depending on the number of design variables and computational capacity. Figure 7 uses Δ_1 to represent $\Delta(\boldsymbol{x}_{Ub}\text{-}\boldsymbol{x}_{Lb})$.

(3) *Collaboration Model and Feasibility Check* – steps 5 and 6: p sample points from the Global Sampling and p_3 points from the Adaptive Sampling are separately approximated with RBF approximation based on the database of experimental points by

$$\overline{y}_{q,i} = \overline{\mathrm{Y}}_i\left(\tilde{\boldsymbol{x}}_{q,i}\right), i = 1, ..., n, \left(q = 1, ..., p \text{ or } p_3\right) \tag{17}$$

$$\overline{\overline{y}}_{q,i} = \overline{\overline{\mathrm{Y}}}_i\left(\boldsymbol{x}_{q,i}, \boldsymbol{x}_{q,csi}, \overline{\boldsymbol{y}}_{q,ci}\right), i = 1, ..., n, \left(q = 1, ..., p \text{ or } p_3\right) \tag{18}$$

Points that cannot yield matched state parameters y by calling Eq. (2) are deemed infeasible subject to SA/MDA. The matching between coupled state parameters is maintained by the Collaboration Model, which filters out infeasible points subject to SA/MDA based on an interdisciplinary discrepancy distribution of sample points. The interdisciplinary discrepancy of each point is calculated by

$$D_q = \sum_{i=1}^{n} \left| \overline{y}_{q,i} - \overline{\overline{y}}_{q,i} \right|, q = 1, ..., p \text{ or } p_3 \tag{19}$$

The Collaboration Model shows a distribution of the interdisciplinary discrepancy subject to SA/MDA over all sample points by Eq. (19). Sequentially, the constraint check is implemented by

$$\overline{\boldsymbol{g}}_q = \overline{\mathbf{G}}\left(\boldsymbol{x}_q, \overline{\boldsymbol{y}}_q\right), q = 1, ..., p \text{ or } p_3 \tag{20}$$

$$\overline{\overline{\boldsymbol{g}}}_q = \overline{\overline{\mathbf{G}}}\left(\boldsymbol{x}_q, \overline{\overline{\boldsymbol{y}}}_q\right), q = 1, ..., p \text{ or } p_3 \tag{21}$$

Sample points violating constraints determined by either Eq. (20) or Eq. (21) or both are discarded. This is a conservative way to make sure that selected sample points are feasible subject to the constraints. The numbers of remaining sample points are p_1 and p_4, inherited from the Global Sampling and the Adaptive Sampling, respectively.

(4) In steps 7 – 9, the approximated objective function, $\tilde{f}$, of the p_4 samples will be evaluated given design variables and $\bar{\boldsymbol{y}}$. For a minimization problem, a sample point with the smallest value of $\tilde{f}$ is selected as one of the new experiments, from the p_4 points given by the Adaptive Sampling, and is called a Local Seed.

(5) *Global Optimizer – MPS* – step 10: Global Seeds (new experiments) chosen from p_1 points are determined by the MPS method. Two guidance functions are built for this process.

a) In steps 10.1 and 10.2, p_1 points are sorted in an ascending order in terms of the value of the interdisciplinary discrepancy given by Eq. (19). Guidance Function I is formed by

$$GD\left(\boldsymbol{x}_q\right) = \sum_{i=1}^{n} \left| \bar{y}_{q,i} - \bar{\bar{y}}_{q,i} \right|, \; q = 1, ..., \; p_1 \tag{22}$$

Then Eq. (22) is cumulated over p_1 sample points by

$$CD\left(\boldsymbol{x}_q\right) = \frac{\sum_{j=1}^{q} GD\left(\boldsymbol{x}_j\right)}{\sum_{i=1}^{p_1} GD\left(\boldsymbol{x}_i\right)}, \; q = 1, ..., \; p_1 \tag{23}$$

Finally, p_2 points, e.g., 200, are statistically selected from a modified Guidance Function I given by

$$\overline{CD}\left(\boldsymbol{x}_q\right) = \left(CD\left(\boldsymbol{x}_q\right)\right)^{SP_1}, \; q = 1, ..., \; p_1 \tag{24}$$

The purpose of Guidance Function I is to select p_2 possibly feasible points subject to SA/MDA and constraints.

b) In steps 10.3 - 10.5, the approximate objective values, $\tilde{f}\left(\boldsymbol{x}\right)$, of all p_2 points are calculated. These p_2 points are sorted in an ascending order in terms of $\tilde{f}\left(\boldsymbol{x}\right)$ values. The Guidance Function II is built up by

$$GF\left(\boldsymbol{x}_q\right) = \max\left(\left.\tilde{f}\left(\boldsymbol{x}_i\right)\right|_{i=1,\ldots,\,p_2}\right) - \tilde{f}\left(\boldsymbol{x}_q\right),\ q = 1,\ldots,\ p_2 \tag{25}$$

Then Eq. (25) is cumulated over p_2 points by

$$CF\left(\boldsymbol{x}_q\right) = \frac{\sum_{j=1}^{q} GF\left(\boldsymbol{x}_j\right)}{\sum_{i=1}^{p_2} GF\left(\boldsymbol{x}_i\right)},\ q = 1,\ldots,\ p_2 \tag{26}$$

Finally, k points, e.g. 3, are selected statistically as the new experimental points (Global Seeds), from a modified Guidance Function II defined by

$$\overline{CF}\left(\boldsymbol{x}_q\right) = \left(CF\left(\boldsymbol{x}_q\right)\right)^{SP_2},\ q = 1,\ldots,\ p_2 \tag{27}$$

The sample point with the smallest value of $\tilde{f}\left(\boldsymbol{x}\right)$ in p_2 point should be included in the k selected sample points since this one is promising.

(6) All selected sample points will be passed to the SA/MDA module to calculate the state parameters, $\boldsymbol{y}$, as well as the objective function, f, in step 2. The experimental points which satisfy SA/MDA are saved into the database of experimental points to improve the quality of the next RBF approximation. The CPM process can be stopped if there is no further improvement of f after a certain number of consecutive CPM iterations, e.g., 6.

In summary, the Collaboration Model allows CPM to extract useful information in compliance with SA/MDA. Based on the Collaboration Model, CPM uses selected sample points to tune the RBF approximation model, and consequently the RBF approximation model gradually improves its accuracy. The MPS method retains the possibility to pursue the global optimum solution. In the next section, some test cases are solved with CPM.

VI. Test Problems and Discussion

Three numerical test cases and one engineering application are solved with CPM. The first numerical test case is formulated by the authors by placing two coupled state parameters as system-variables into the well-known six-hump camel-back problem. Test Cases 2 and 3 are obtained from Ref. 35. Finally, a power converter problem is solved as a benchmark MDO problem.[36,37] According to Figure 6 and Figure 7, the CPM process starts with initial feasible experiments for solving all test cases. Only in Test Case 2 the Adaptive Sampling module is applied. To observe the robustness and consistency of CPM, 10 independent runs have been carried out for each test case. The convergence tolerance of the 'fsolve' function in MATLAB® 6.0 (Ref. [37]) for solving the SA/MDA is set to 10^{-4} in Test Cases 1, 2, and 4, and 10^{-7} in Test Case 3. For each test case, one of the 10 independent runs is randomly chosen for plotting the cumulative number of the SA/MDA evaluations over CPM iterations.

A. Test Case 1

$$\begin{aligned} &\min f = 4y_1^2 - 2.1y_1^4 + \frac{y_1^6}{3} + y_1y_2 - 4y_2^2 + 4y_2^4 \\ &\text{subject to: } y_1 = x_1 + x_2 - 2 + \left(y_2/1.5\right)^4 \\ &\qquad y_2 = x_3 + x_4 - 2 + \left(y_1/1.8\right)^4 \\ &\qquad y_1 \le 1.2 \\ &\qquad y_2 \le 1.0 \\ &\qquad 1 \le x_1, x_2, x_3, x_4 \le 1.9 \end{aligned} \tag{28}$$

Based on intensive enumeration by calling the SA/MDA in Eq. (28), a feasible region (plotted with "dots" and two straight lines), subject to both the SA/MDA and constraints in the design space of the six-camel hump-back problem, is shown in Figure 9. Also, Figure 9 shows the optimization process of CPM by experimental points marked with different signs. The optimum solution of Test Case 1 should be located in the feasible region in compliance with its SA/MDA and constraints, and it should be as close as possible to $f = -0.1$ according to the contour of f in Figure 9. Speed factors of the first and the second Guidance Functions are fixed as 0.51 and 0.07, respectively. At the end of each CPM iteration, 4 sample points (Global Seeds) are selected. Results of Test Case 1 are shown in Table 3. All runs start with 5 feasible experiments. Runs 1-9 are stopped if the value of f is less than –0.9. In particular, the optimization process of Run 10 is terminated when no further improvement of f occurs after 10 consecutive CPM iterations. The convergence history of the objective function for Runs 1-10 is plotted in Figure 10.

According to the objective function contour of the six-camel hump-back problem in Figure 9, the optimum is reached successfully.

B. Test Case 2

$$
\begin{aligned}
&\min f = y_1 + \left(x_2 - 2\right)^2 + x_3 - 2 + e^{-y_2} \\
&\text{subject to: } y_1 = x_1^{\,2} + x_2 + x_3 - 4 - 0.2y_2 \\
&\qquad y_2 = x_1 + x_3 - 2 + \sqrt{y_1} \\
&\qquad 0 \le x_1 \le 7 \textit{ and } 2 \le x_2, x_3 \le 7 \\
&\qquad y_1 / 8 - 1 \ge 0 \textit{ and } 1 - y_2 / 10 \ge 0
\end{aligned}
\tag{29}
$$

Speed factors of the first and the second Guidance Functions are fixed as 1 and 0.41, respectively. At the end of each CPM iteration, 3 sample points (1 Local Seed and 2 Global Seeds) are selected. Results are listed in

Table 4. Runs 1-3 are stopped if the value of f is less than 8.08; Runs 4-6 are stopped if the value of f is less than 8.04; and Runs 7 – 9 are terminated after 6 consecutive CPM iterations with no further improvement of the value of f. All runs start with 5 random feasible experiments. The Adaptive Sampling module is applied in Runs 1-9 by setting $\Delta = 5\%$. It is observed that the Adaptive Sampling is especially efficient when the system objective function f is sensitive to the variation of its design variables. Comparisons are given between Runs 1-9 and Run 10, which does not apply Adaptive Sampling and it is stopped if the value of f is less than 8.08. Apparently, Run 10 has the worst optimum value with the highest number of calls to the SA/MDA. The convergence history of f of Runs 7-9 is shown in Figure 11.

C. Test Case 3

$$\begin{aligned} &\min f = \frac{y_1^{\,2}}{x_1} + y_2^{\,2} - x_2 \\ &\text{subject to: } y_1 = \frac{x_1 y_2 y_3^{\,2}}{x_2 y_4},\ y_2 = \sqrt{\frac{x_1 y_3}{x_2}},\ y_3 = \frac{y_1 y_4}{2 x_1 y_2} \\ &\qquad y_4 = \frac{x_1 y_3^{\,2}}{x_2^{\,2}},\ h_1 = y_4 - y_3 - 2 = 0 \\ &\qquad g_1 = y_2^{\,2} + 1 - x_1 \geq 0,\ 0 < x_i \leq 1,\ i = 1,2 \end{aligned} \tag{30}$$

Speed factors of the first and the second Guidance Functions are set to 0.51 and 0.81, respectively. Upper bounds of the design variables are assigned by the authors. At the end of each CPM iteration, 5 sample points (Global Seeds) are selected. The SA/MDA solver within CPM is applied to evaluate the optimal solution given by Ref. 35 to verify the accuracy of the solver. For the given design variable set, the optimal objective function value is the same as reported in Ref. 35, which is 2.984 as shown in Table 5 (the optimum values of $\boldsymbol{y}$ are not available in Ref. 35). All runs are terminated after 6 consecutive CPM iterations without further improvement of f. All of the 10 runs start with 3 random feasible experiments. Results by running CPM are shown in

Table 6. The optimal function values obtained are in the neighborhood of 1.0, which is better than 2.984, given by the CSSO method in Ref. 35. It is very difficult to maintain the feasibility of samples subject to SA/MDA in this case, since the SA/MDA in Eq. (30) is over constrained by an equality constraint. The trend of the objective function of Runs 1-10 is plotted in Figure 12. The difficulty of achieving feasible sample points, raised by the equality constraint, results in large computational effort for initialization and an early stop of the optimization process according to the optimization convergence criterion.

D. Test Case 4

The power converter problem comprises a coupling between an electrical subsystem and a loss subsystem. An optimal power stage design is essential to the development of a quality power converter. The power stage design dominates the overall efficiency, size, and weight of the power converter. The objective of the power converter problem is to minimize the weight. The problem consists of six design variables and twelve state variables, of which four define constraints. All constant values are taken from Ref. 37. A schematic of the power converter problem is shown in Figure 13, and the geometry of the transformer core is shown in Figure 14. The formulation of the power converter problem is defined by

$$y_1 = f(x) = W_c + W_w + W_{cap} + W_{hs} \tag{31}$$

Subject to:

Electrical Design State Analysis duty cycle: $y_3 = \dfrac{EO}{\left(\dfrac{y_2 EI}{2(XN)}\right)}$

minimum duty cycle: $y_4 = \dfrac{EO}{\left(\dfrac{y_2 EIMAX}{2XN}\right)}$

inductor resistance: $y_5 = \dfrac{XMLTx_2(RO)}{x_3}$,

where $XMLT = 2x_1(1 + K_1)FC$

core cross-sectional area: $y_6 = K1|x_1|x_1$

magnetic path length: $y_7 = \dfrac{\pi}{2}x_1$

$$\text{inductor value: } y_8 = \frac{(EO + VD)(1 - y_3)}{y_6 x_2 (FR)}$$

Loss Design State Analysis

$$\text{circuit efficiency: } y_2 = \frac{PO}{PS + PQ + PD + POF + PXFR}$$

Fill Window Constraint

$$g_1 = WA - \frac{x_3 x_2}{FW} + (-WBOB) x_6 K_2 \geq 0,$$

$$\text{where } WA = K_2 x_6 |x_6|$$

Ripple Specification

$$g_2 = \frac{VR - DELI(ESR)}{EO} \geq 0, \text{ where } DELI = \frac{(EO + VD)(1 - y_3)}{x_4 FR}$$

Core Saturation $g_3 = BSP - \frac{x_4 (XIMAX)}{y_6 x_2} \geq 0,$

$$\text{where } XIMAX = \frac{PO}{EO} + \frac{(EO + VD)(1 - y_4)}{2 x_4 FR}$$

Minimum Inductor Size for Continuous Mode at EIMAX and POMIN

$$g_4 = x_4 - XLCRIT \geq 0,$$

$$\text{where } XLCRIT = \frac{(EO + VD)(1 - y_4) EO}{2(POMIN) FR}$$

where $W_c = |DIy_6 (ZP_1 + y_7)|$, $ZP_1 = 2(1 + K_2) x_6$, $W_w = |(XMLT)(DC) x_3 x_2|$, $XMLT = 2x_1(1 + K_1)FC$,

$W_{cap} = |(DK_5) x_5|$, and $W_{hs} = \left| \frac{PO}{KH} \left(\frac{1}{y_2} - 1 \right) \right|$.

The power converter problem has 6 design variables, as shown in Table 7. Relatively large upper bounds of all design variables and the lower bound of x_4 are assigned by the authors, by referring to the optimum solution and the lower bounds of design variables from Refs. 36 and 37. The problem is mainly dominated by the couplings among y_2, y_3 and y_8, and the explicit dependency matrix is shown Table 8. Speed factors of the first and the second

Guidance Functions are fixed as 1 and 0.00011, respectively. At the end of each CPM iteration, 2 sample points (Global Seeds) are selected. Similar to Test Case 3, the SA/MDA solver within CPM is applied to evaluate the optimum solution in Ref. 36 to verify the accuracy of the solver. As shown in Table 9, CPM has the same accuracy as the CSSO method in Ref. 36. After the verification, 10 independent optimization runs are carried out with CPM, and terminated when no further improvement of f after 6 consecutive CPM iterations, as shown in Table 10. All runs start with 4 random feasible experiments. The convergence of f of Runs 1-10 is plotted in Figure 15. For Run 4 (with the highest number of calls to the SA/MDA in Table 10), the cumulative number of SA/MDA at each CMP iteration step is shown in Figure 16.

According to Ref. 36, the optimum solution (f = 1.48) is given by CSSO with 54 'Design Point System Iterations', and a 'Design Point System Iteration' refers to a call to the SA/MDA, CPM is thus more efficient than CSSO for solving the power converter problem, based on the results in Tables 9-10.

E. Discussion

For the implementation of MPS, if the Guidance Function I (Eq. (24)) is sped up intensively by applying a small value of SP_1, e.g., SP_1 = 0.01, new sample points given from the current CPM iteration to the next one are most likely feasible. An aggressive (small) speed factor can increase the efficiency of MPS but may only lead to a local optimum; and a large speed factor value could slow down the optimization procedure. Based on the feedback from the last CPM iteration, the speed factor could be dynamically adjusted by designers' intervention. For example, the value of the speed factor should be reduced if the value of f is not improved after several consecutive CPM iterations and the number of feasible experiments is larger than that of infeasible experiments at each CPM iteration. In this work for fair comparison, the speed factors are fixed throughout one optimization process and fixed for a number of independent runs. The efficiency of CPM can be potentially further improved by dynamically tuning the speed factors.

In this work, CPM starts with feasible experimental points subject to both SA/MDA and constraints. A common problem from all results is that CPM spent a lot of efforts in generating initial feasible experiments. As the number of state parameters and design variables increase, initialization could become a problem, so a good initialization procedure is important. A strategy is tested to generate feasible experiments by giving a small offset to the design variables of the last feasible experimental point. Although this strategy has been shown successful, it does not

guarantee that feasible experiments will be generated. A new initialization process, based on feasible experimental points subject to SA/MDA but not necessarily to constraints, has been applied to a conceptual aircraft design problem.[27,39] More feasible experiments subject to both SA/MDA and constraints are expected to be created after the initialization step to replace the infeasible experiments subject to constraints in the database of experiments. This is more efficient than the current initialization process. Also for engineering problems, experimental data and other related experience can partly alleviate such a difficulty in initialization.

The efficiency and capability of sampling-based optimization methods are dependent on the range and number of design variables. As the range and number of design variables become large, CPM encounters difficulties caused by limited sample size, which can not effectively cover the entire design space. The Adaptive Sampling showed its advantage in this regard when solving Test Case 2. For large-scale design problems, the key to the sampling-based optimization methods is to effectively reduce the number and range of the design variables, while maintaining the optimization progress. Due to the nature of sampling, the capability and efficiency of CPM can be improved by applying parallel computing for generating a very large number of sample points.

It is observed that the Collaboration Model is effective for collaborating coupled subsystems. For MDO problems, the number of coupled state parameters is usually relatively low when compared with design variables. Based on this observation, the Collaboration Model could be still effective in dealing with a high degree of coupling. To test applicability of CPM in this regard, a conceptual aircraft design problem involving 10 design variables, 12 constraints, and 3 nonlinear coupled disciplines was solved efficiently with CPM.[27]

CPM relies on SA/MDA rather than sensitivity analyses. From this perspective, CPM is an All-in-One/MDF-like MDO approach, which aims to reduce the total number of calls to SA/MDA. Its efficiency has been demonstrated through comparisons with the All-in-One/MDF in Refs. 27 and 39. In general, CPM has the same level of applicability for solving MDO problems as the All-in-One/MDF approach. The efficiency of CPM comes from an integration of collaboration modeling, metamodeling, and sampling-based optimizers. A global search algorithm, MPS, is applied in CPM. As MPS is a sampling-based search algorithm and only the number of expensive function evaluation is used as the efficiency measure (the cost of evaluating metamodels is negligible compared to the cost of expensive function evaluation), MPS is thus an efficient global search scheme for expensive black-box functions. Similarly, CPM is a sampling-based MDO approach for expensive SA/MDA processes. It selects promising points from a sample pool, which are determined from search or optimization methods, and only a few selected sample

points are evaluated expensively. Therefore as a global search scheme, CPM still demonstrates high efficiency from the perspective of the total number of expensive SA/MDA processes.

VII. Conclusions

This paper proposed the Collaboration Model (CM), which is constructed by two mutually dependent approximation functions. The CM reflects both the physical and mathematical characteristics of couplings and effectively coordinates coupled subsystems for solving test cases. Based on the CM, the Collaboration Pursuing Method (CPM), as a sampling-based MDO method, is developed. CPM uses the Mode Pursing Sampling (MPS) method to search for the global optimum, and the Adaptive Sampling strategy to enhance its capability to converge to local optimum solutions. Four test cases have been successfully and robustly solved with CPM. Future work will be focused on investigating the applicability and efficiency of CPM for MDO problems with a large scale of design variables and a fairly large number of state parameters.

Acknowledgments

Support of this research from the Natural Sciences and Engineering Research Council (NSERC) of Canada is gratefully acknowledged. Also, the assistance of Mr. Shan, S. is gratefully acknowledged.

References

[1]Wang, D., Naterer, G. F., and Wang, G. G., "Adaptive Response Surface Method for Thermal Optimization: Application to Aircraft Engine Cooling System," AIAA-2002-3000, *AIAA / ASME 8th Joint Thermophysics and Heat Transfer Conference*, St. Louis, MO, June 24–27, 2002.

[2]Wang, D., Naterer, G.. F., Wang, G. G., "Thermofluid Optimization of a Heated Helicopter Engine Cooling Bay Surface," *Canadian Aeronautics and Space Journal*, Vol. 49, June 2003, pp. 73–86.

[3]Schrage, D., Beltracchi, T., Berke, L., Dodd, A., Niedling, L, and Sobieszczanski-Sobieski, J., "Current State of the Art on Multidisciplinary Design Optimization (MDO)," An AIAA White Paper, ISBN 1-56347-021-7, September 1991.

[4]Sobieszczanski-Sobieski J., and Haftka, R. T., "Multidisciplinary Aerospace Design Optimization: Survey of Recent Developments," *34th AIAA Aerospace Sciences Meeting and Exhibit*, Reno, Nevada, AIAA-96-0711, January 15–18, 1996, pp. 32.

[5]Balling, R. J., and Sobieszczanski-Sobieski, J., "Optimization of Coupled Systems: a Critical Overview of Approaches," *AIAA Journal*, Vol. 36, No. 1, Jan. 1996, pp. 6–17.

[6]Kodiyalam, S., and Sobieszczanski-Sobieski, J., "Multidisciplinary Design Optimization – Some Formal Methods, Framework Requirements, and Application to Vehicle Design," *International Journal of Vehicle Design*, special issue: Vol. 25, No. 1-2, 2001, pp. 3-22.

[7]Balling, R. J., and Wilkinson, C. A., "Execution of Multidisciplinary Design Optimization Approaches on Common Test Problems," *AIAA Journal*, Vol. 35, No. 1, Jan. 1997, pp. 178–186.

[8]Kodiyalam, S., "Evaluation of Methods for Multidisciplinary Design Optimization (MDO), Phase I," NASA/CR-1998-208716, Sept. 1998.

[9]Kodiyalam, S., "Evaluation of Methods for Multidisciplinary Design Optimization (MDO), Phase II," NASA/CR-2000-210313, Nov. 2000.

[10] Wang, D., Naterer, G.. F., and Wang, G. G., "Boundary Search and Decomposition Method for MDO Problems with a Convex State Parameter Region," AIAA-2005-0128, *43rd Aerospace Sciences Meeting and Exhibit*, Reno, Nevada, Jan. 10–13, 2005.

[11] Burden, R. L., and Faires, J. D., *Numerical Analysis*, 7th ed., ISBN: 0534382169, Brooks/Cole, Pacific Grove, CA, 2000, Chapters 7 and 10.

[12] Alexandrov, N. M., and Lewis, R. M., "Algorithmic Perspectives on Problem Formulations in MDO," *8th AIAA/USAF/NASA/ISSMO Symposium on Multidisciplinary Analysis & Optimization*, AIAA-2000-4719, Long Beach, CA, September 6–8, 2000.

[13] Sobieszczanski-Sobieski, J., "Optimization by Decomposition: a Step from Hierarchic to Non-Hierarchic Systems," *Second NASA/Air Force Symposium on Recent Advances in Multidisciplinary Analysis and Optimization*, Hampton, Virginia, Sept. 1988, or NASA conference publication, CP-3031, Part 1.

[14] Hajela, P., Bloebaum, C. L., and Sobieszczanski-Sobieski, J., "Application of Global Sensitivity Equations in Multidisciplinary Aircraft Synthesis," *AIAA Journal*, Vol. 27, No. 12, Dec. 1990, pp. 1002–1010.

[15] Sobieszczanski-Sobieski, J., "Sensitivity of Complex, Internally Coupled Systems," *AIAA Journal*, Vol. 28, No. 1, Jan. 1990, pp. 153–160.

[16] Renaud, J. E., and Gabriele, G. A., "Sequential Global Approximation in Non-Hierarchic System Decomposition and Optimization," *Advances in Design Automation*, *Design Automation and Design Optimization*, ASME Publication DE-Vol. 32-1, G. Gabriele (Ed.), pp. 191-200, 19th Design Automation Conference, Miami, Florida, Sept. 22-25, 1991.

[17] Renaud, J. E., and Gabriele, G. A., "Improved Coordination in Non-Hierarchic System Optimization," *AIAA Journal*, Vol. 31, No. 12, Dec. 1993, pp. 2367–2373.

[18] Sobieszczanski-Sobieski, J., Agte, J. S., and Sandusky Jr., R., "Bilevel Integrated System Synthesis," *AIAA Journal*, Vol. 38, No. 1, Jan. 2000, pp. 164–172.

[19] Kodiyalam, S., and Sobieszczanski-Sobieski, J., "Bilevel Integrated System Synthesis with Response Surface," *AIAA Journal*, Vol. 38, No. 8, Aug. 2000, pp. 1479–1485.

[20] Kroo, I., Altus, S., Braun, R., Gage, P., and Sobieski, I., "Multidisciplinary Optimization Methods for Aircraft Preliminary Design," *5th AIAA/USAF/NASA/ISSMO Symposium on Multidisciplinary Analysis and Optimization*, AIAA-94-4325, Panama City Beach, FL., Vol. 1, 1994, pp. 697–707.

[21] Braun, R. D., and Kroo, I. M., "Development and Application of the Collaborative Optimization Architecture in a Multidisciplinary Design Environment," *Multidisciplinary Design Optimization: State of the Art*, N. M. Alexandrov and M. Y. Hussaini, eds., *SIAM*, 1997, pp. 98–116.

[22] Braun, R., Gage, P., Kroo, I., and Sobieski, I., "Implementation and Performance Issues in Collaborative Optimization," *6th AIAA/NASA/ISSMO, Symposium on Multidisciplinary Analysis and Optimization*, AIAA-96-4017-CP, Bellevue, WA, Sept. 4–6, 1996.

[23] Sobieski, I. P., and Kroo, I. M., "Collaborative Optimization Using Response Surface Method," *AIAA Journal*, Vol. 28, No. 10, Oct. 2000, pp. 1931–1938.

[24] Alexandrov, N. M., and Lewis, R. M., "Analytical and Computational Aspects of Collaborative Optimization," NASA TM-2000-210104, 2000.

[25] Alexandrov, N. M., and Lewis, R. M., "Comparative Properties of Collaborative Optimization and Other Approaches to MDO," NASA/CR-1999-209354, *ICASE Report*, ICASE Report No. 99-24, July 1999.

[26] Wang, D., Wang, G. G., and Naterer, F. G., "Collaboration Pursuing Method for MDO Problems," *1st AIAA Multidisciplinary Design Optimization Specialist Conference*, AIAA-2005-2204, Austin, Texas, April 18–21, 2005.

[27] Wang, D., "Multidisciplinary Design Optimization with Collaboration Pursuing and Domain Decomposition: Application to Aircraft Design," Ph.D. Dissertation, Mechanical and Manufacturing Dept., University of Manitoba, Manitoba, Canada, May 2005.

[28] Wang, D., "Study of Collaboration Model", Technical Report, University of Manitoba, Winnipeg, Manitoba, Canada, May 2005.

[29] Micchelli, C. A., "Interpolation of Scattered Data: Distance Matrices and Conditionally Positive Definite Functions," *Constructive Approximation*, Vol. 2, No. 1, Dec. 1986, pp. 11–22

[30] Haykin, S., *Neural Networks – A Comprehensive Foundation*, 2nd ed., Prentice Hall, New Jersey, 1999, Chap. 5.

[31] Wang, L., Shan, S., and Wang, G. G., "Mode-Pursuing Sampling Method for Global Optimization on Expensive Black-Box Functions," *Journal of Engineering Optimization*, Vol. 36, No. 4, August 2004, pp. 419–438.

[32] Shan, S., and Wang, G. G., "An Efficient Pareto Set Identification Approach for Multi-objective Optimization on Black-box Functions", *Transactions of the ASME, Journal of Mechanical Design*, Vol. 127, No. 5, 2005, pp. 866–874.

[33] Moré, J.J. and D.C. Sorensen, "Computing a Trust Region Step," *SIAM Journal on Scientific and Statistical Computing*, Vol. 4, No. 3, 1983, pp. 553–572.

[34] Pérez, V. M. and Renaud, J. E., "Adaptive Experimental Design for Construction of Response Surface Approximations," *42nd AIAA/ASME/ASCE/AHS/ASC Structures, Structural Dynamics, and Materials Conference*, AIAA-2001-1622, Seattle, WA, April 16–19, 2001.

[35] Tappeta, R., Nagendra, S., Renaud, J. E., and Badhrinath, K., "Concurrent Sub-Space Optimization (CSSO) MDO Algorithm in iSIGHT, CSSO in iSIGHT: Validation and Testing," GE Research & Development Center, 97CRD186, Class 1, Jan. 1998.

[36] Kott, G., Gabriele, G. A., and Korngold, J., "Application of Multidisciplinary Design Optimization to the Power Stage Design of A Power Converter," *ASME, Advances In Design Automation*, Vol. 2, 1993. pp. 359–366.

[37] "Test Suite Problem 2.5, POWER CONVERTER," *NASA MultiDisciplinary Optimization Branch* [online MDOTest Suite],URL:http://mdob.larc.nasa.gov/mdo.test/class2prob5.html [cited 29 July 2004].

[38] MATLAB, Software Package, Ver. 6.0, The MathWorks, Inc., 3 Apple Hill Drive, Natick, MA 01760-2098, U.S.A., 2003.

[39] Wang, D., Wang, G. G., and Naterer, G. F., "Advancement of a Collaboration Pursuing Method," *44rd AIAA Aerospace Sciences Meeting and Exhibit*, AIAA-2006-0730, Reno, Nevada, Jan. 9–12, 2006.

Table 1. Experimental points for the RBF approximation.

Experiments	x_1	x_2	x_3	x_4	y_1	y_2
1	1.306581	1.398711	1.007338	1.048180	0.705300	0.079091
2	1.430430	1.504102	1.106891	1.172904	0.937613	0.353416
3	1.472354	1.571369	1.160585	1.242747	1.058492	0.522912
4	1.047014	1.668556	1.249554	1.318132	0.740550	0.596337
5	1.108217	1.734028	1.302309	1.383587	0.904644	0.749696

Table 2. Experimental points for the study of the Collaboration Model

Experiments	x_1	x_2	y_1	y_2
1	3.503310	0.347277	35.114669	13.745608
2	3.804635	0.199845	54.413245	30.829225
3	3.687938	0.792564	45.010857	22.468824
4	3.750904	0.903145	50.232818	27.700710
5	3.618321	0.841266	40.904291	19.050912
6	3.384046	0.334936	30.655226	10.795279

Table 3. Results of Test Case 1.

No. of Run	# of SA/MDA			Optimum Value of f	Optimum Value of $\boldsymbol{x}$				Optimum Value of $\boldsymbol{y}$	
	Feasible	Infeasible								
		Initial	After Ini.		x_1	x_2	x_3	x_4	y_1	y_2
1	55	2	0	$-9.070575e^{-1}$	1.001897	1.035303	1.526232	1.184495	0.087604	0.710732
2	28	4	0	$-9.111311e^{-1}$	1.002131	1.012684	1.355314	1.264257	0.043922	0.619571
3	20	3	0	$-9.093511e^{-1}$	1.008852	1.008468	1.078122	1.542187	0.046566	0.620309
4	36	1	0	$-9.343211e^{-1}$	1.011585	1.009576	1.594216	1.099452	0.066896	0.693671
5	57	9	0	$-9.154225e^{-1}$	1.000354	1.036599	1.312874	1.370380	0.080004	0.683258
6	26	6	0	$-9.014565e^{-1}$	1.001388	1.042767	1.296005	1.359486	0.080624	0.655495
7	35	12	0	$-9.322473e^{-1}$	1.016560	1.005368	1.489481	1.209155	0.068987	0.698638
8	58	4	0	$-9.409803e^{-1}$	1.000501	1.004792	1.451814	1.194624	0.039787	0.646438
9	29	2	0	$-9.198739e^{-1}$	1.012159	1.021370	1.506066	1.177620	0.076689	0.683689
Ave.				$-9.19e^{-1}$						
σ				$1.37e^{-2}$						
10	79	6	0	$-9.477366e^{-1}$	1.002180	1.005740	1.479164	1.223990	0.056208	0.703155

Table 4. Results of Test Case 2.

No. of Run	# of SA/MDA			Optimum Value of f	Optimum Value of $\boldsymbol{x}$			Optimum Value of $\boldsymbol{y}$	
	Feasible	Infeasible							
		Initial	After Initialization		x_1	x_2	x_3	y_1	y_2
1	21	25	8	8.061338	3.016562	2.042900	2.046421	8.010318	5.893234
2	23	20	9	8.066726	3.004791	2.157272	2.011495	8.027615	5.849590
3	38	17	18	8.030440	3.020825	2.036224	2.019330	8.006974	5.869815
Ave.				8.052835					
σ				0.019581					
4	33	34	10	8.021729	3.020842	2.048775	2.006903	8.009590	5.857867
5	19	5	10	8.028838	3.013692	2.093780	2.005488	8.011675	5.849671
6	68	36	14	8.034520	3.020577	2.071583	2.000979	8.025550	5.854496
Ave.				8.028362					
σ				0.006409					
7	52	24	18	8.014559	3.024412	2.021236	2.007586	8.003674	5.861074
8	49	5	16	8.013545	3.022309	2.029848	2.008772	8.001031	5.859690
9	93	14	17	8.008876	3.026792	2.014285	2.000711	8.005100	5.856832
Ave.				8.0123267					
σ				0.0030311					
10	161	21	7	8.075582	3.011512	2.118991	2.022045	8.036551	5.868438
Results from Ref. 35				8.003	3.025	2.000	2.000		

Table 5. Accuracy Comparison between the CPM and the CSSO applied in Ref. 35.

Method	Optimum Value of f	Optimum Design of $\boldsymbol{x}$ from Ref. 35	Optimum Design of $\boldsymbol{y}$
CPM	2.984	$x_1 = 0.998$ $x_2 = 0.996$	$y_1 = 1.4071$ $y_2 = 1.4128$ $y_3 = 1.9920$ $y_4 = 3.9919$
CSSO in Ref. 35	2.984		N/A

Table 6. Results of Test Case 3.

No. of Run	# of SA/MDA			Optimum Value of f	Optimum Value of $\boldsymbol{x}$	Optimum Value of $\boldsymbol{y}$
	Feasible	Infeasible				
		Initial	After Initialization			
1	40	171	27	0.996646	$x_1 = 0.522049$ $x_2 = 0.072530$	$y_1 = 0.073801$ $y_2 = 1.028952$ $y_3 = 0.147079$ $y_4 = 2.146778$
2	35	218	20	0.938502	$x_1 = 0.447010$ $x_2 = 0.015635$	$y_1 = 0.014464$ $y_2 = 0.976560$ $y_3 = 0.033348$ $y_4 = 2.033509$
3	36	297	2	0.890401	$x_1 = 0.398669$ $x_2 = 0.005149$	$y_1 = 0.004404$ $y_2 = 0.946309$ $y_3 = 0.011567$ $y_4 = 2.011850$
4	43	180	0	1.007149	$x_1 = 0.516492$ $x_2 = 0.020540$	$y_1 = 0.020914$ $y_2 = 1.013332$ $y_3 = 0.040829$ $y_4 = 2.040768$
5	35	350	44	1.031431	$x_1 = 0.562961$ $x_2 = 0.121428$	$y_1 = 0.128897$ $y_2 = 1.059881$ $y_3 = 0.242341$ $y_4 = 2.242294$
6	18	264	0	0.966130	$x_1 = 0.477408$ $x_2 = 0.024440$	$y_1 = 0.023621$ $y_2 = 0.994687$ $y_3 = 0.050652$ $y_4 = 2.050567$
7	20	295	25	0.983973	$x_1 = 0.499534$ $x_2 = 0.036815$	$y_1 = 0.036586$ $y_2 = 1.009014$ $y_3 = 0.075030$ $y_4 = 2.074819$
8	28	69	30	0.973706	$x_1 = 0.488703$ $x_2 = 0.034050$	$y_1 = 0.033357$ $y_2 = 1.002736$ $y_3 = 0.070074$ $y_4 = 2.069790$
9	15	308	20	0.991809	$x_1 = 0.515382$ $x_2 = 0.062673$	$y_1 = 0.063319$ $y_2 = 1.023085$ $y_3 = 0.127323$ $y_4 = 2.127136$
10	16	46	45	1.129521	$x_1 = 0.628626$ $x_2 = 0.252015$	$y_1 = 0.282756$ $y_2 = 1.119979$ $y_3 = 0.502852$ $y_4 = 2.502753$
Ave.				0.990927		
σ				0.062325		

Table 7. Design variables of the power converter problem.

Variable	Name	Description	Range	
			Lower Bound	Upper Bound
x_1	C_w	Core center leg width	0.001	0.1
x_2	Turns	Inductor turns	1.0	10.
x_3	A_{cp}	Copper size	$7.29e^{-8}$	$1.0e^{-5}$
x_4	L_f / PINDUC	Inductance	$1.0e^{-6}$	$1.0e^{-5}$
x_5	C_f	Capacitance	$1.e^{-5}$	0.01
x_6	W_w	Core window width	0.001	0.01

Table 8. Dependency matrix of the power converter problem.

	y_1	y_2	y_3	y_4	y_5	y_6	y_7	y_8	x_1	x_2	x_3	x_4	x_5	x_6
y_1 / f		x				x	x		x	x	x		x	X
y_2			x		x	x	x	x				x	x	X
y_3		x												
y_4		x												
y_5									x	x	x			
y_6									x					
y_7									x					
y_8			x			x				x				
g_1										x	x			x
g_2			x									x		
g_3				x		x				x		x		
g_4				x								x		

Table 9. Accuracy Comparison between CPM and the CSSO method applied in Ref. 36.

Method	Optimum Value of f	Optimum Design of $\boldsymbol{x}$ from Ref. 36	Optimum Design of $\boldsymbol{y}$
CPM	1.4856	$x_1 = 0.0191$ $x_2 = 4.91$ $x_3 = 0.00000677$ $x_4 = 0.00000524$ $x_5 = 0.00263$ $x_6 = 0.00759$	$y_2 = 0.8302$ $y_3 = 0.5929$ $y_4 = 0.4535$ $y_5 = 0.0018$ $y_6 = 0.0003648$ $y_7 = 0.0300$ $y_8 = 0.0128$
CSSO used in Ref. 36	1.48		$y_2 = 0.830$ $y_3 = 0.593$ $y_4 = 0.453$ $y_5 = 0.00182$ $y_6 = 0.000367$ $y_7 = 0.0301$ $y_8 = 0.0128$

Table 10. Results of Test Case 4.

No. of Run	# of SA/MDA			Optimum Value of f	Optimum Value of $\boldsymbol{x}$	Optimum Value of $\boldsymbol{y}$
	Feasible	Infeasible				
		Initial	After Ini.			
1	35	1	3	1.40026	$x_1 = 0.011965$ $x_2 = 5.137405$ $x_3 = 0.000008$ $x_4 = 0.000002$ $x_5 = 0.008793$ $x_6 = 0.008656$	$y_2 = 0.841751$ $y_3 = 0.584688$ $y_4 = 0.032096$ $y_5 = 0.447247$ $y_6 = 0.001006$ $y_7 = 0.000143$ $y_8 = 0.018794$
2	30	3	1	1.46960	$x_1 = 0.018990$ $x_2 = 3.261643$ $x_3 = 0.000007$ $x_4 = 0.000002$ $x_5 = 0.006239$ $x_6 = 0.007036$	$y_2 = 0.840183$ $y_3 = 0.585882$ $y_4 = 0.019873$ $y_5 = 0.448082$ $y_6 = 0.001126$ $y_7 = 0.000361$ $y_8 = 0.029829$
3	20	0	7	1.46435	$x_1 = 0.015288$ $x_2 = 4.819028$ $x_3 = 0.000007$ $x_4 = 0.000003$ $x_5 = 0.007675$ $x_6 = 0.007685$	$y_2 = 0.836584$ $y_3 = 0.588444$ $y_4 = 0.020638$ $y_5 = 0.450009$ $y_6 = 0.001384$ $y_7 = 0.000234$ $y_8 = 0.024015$
4	33	6	2	1.48278	$x_1 = 0.019377$ $x_2 = 2.581968$ $x_3 = 0.000009$ $x_4 = 0.000002$ $x_5 = 0.007388$ $x_6 = 0.008073$	$y_2 = 0.845515$ $y_3 = 0.582134$ $y_4 = 0.024302$ $y_5 = 0.445256$ $y_6 = 0.000766$ $y_7 = 0.000375$ $y_8 = 0.030437$
5	22	31	0	1.44344	$x_1 = 0.017046$ $x_2 = 3.373527$ $x_3 = 0.000008$ $x_4 = 0.000003$ $x_5 = 0.007254$ $x_6 = 0.008487$	$y_2 = 0.843580$ $y_3 = 0.583488$ $y_4 = 0.023968$ $y_5 = 0.446277$ $y_6 = 0.000903$ $y_7 = 0.000291$ $y_8 = 0.026776$
6	25	0	4	1.49415	$x_1 = 0.020723$ $x_2 = 3.178963$ $x_3 = 0.000006$ $x_4 = 0.000004$ $x_5 = 0.004352$ $x_6 = 0.005940$	$y_2 = 0.833817$ $y_3 = 0.590396$ $y_4 = 0.016946$ $y_5 = 0.451502$ $y_6 = 0.001568$ $y_7 = 0.000429$ $y_8 = 0.032552$
7	29	2	3	1.44674	$x_1 = 0.016082$ $x_2 = 5.453818$ $x_3 = 0.000007$ $x_4 = 0.000003$ $x_5 = 0.004478$ $x_6 = 0.007960$	$y_2 = 0.832009$ $y_3 = 0.591687$ $y_4 = 0.016351$ $y_5 = 0.452484$ $y_6 = 0.001694$ $y_7 = 0.000259$ $y_8 = 0.025262$
8	26	9	3	1.39168	$x_1 = 0.012810$ $x_2 = 5.567491$ $x_3 = 0.000008$ $x_4 = 0.000002$ $x_5 = 0.006761$ $x_6 = 0.009895$	$y_2 = 0.840247$ $y_3 = 0.585794$ $y_4 = 0.025761$ $y_5 = 0.448048$ $y_6 = 0.001109$ $y_7 = 0.000164$ $y_8 = 0.020122$
9	27	5	0	1.43167	$x_1 = 0.012973$ $x_2 = 7.524132$ $x_3 = 0.000008$ $x_4 = 0.000003$ $x_5 = 0.005366$ $x_6 = 0.009920$	$y_2 = 0.832640$ $y_3 = 0.591244$ $y_4 = 0.018234$ $y_5 = 0.452141$ $y_6 = 0.001669$ $y_7 = 0.000168$ $y_8 = 0.020378$
10	29	1	0	1.396361	$x_1 = 0.015761$ $x_2 = 3.054849$ $x_3 = 0.000007$ $x_4 = 0.000002$ $x_5 = 0.007356$ $x_6 = 0.007650$	$y_2 = 0.843796$ $y_3 = 0.583243$ $y_4 = 0.031227$ $y_5 = 0.446163$ $y_6 = 0.000866$ $y_7 = 0.000248$ $y_8 = 0.024757$
Ave.				1.442103		
σ				0.036716		

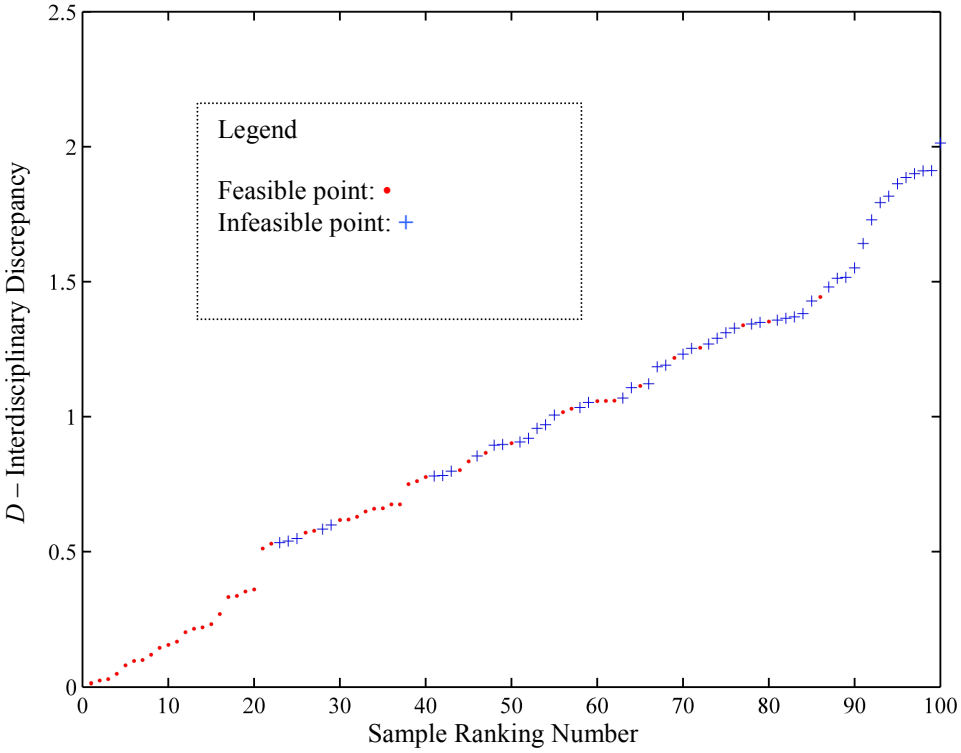

Figure 1. Distribution of *D* - interdisciplinary discrepancy of 100 random sample points.

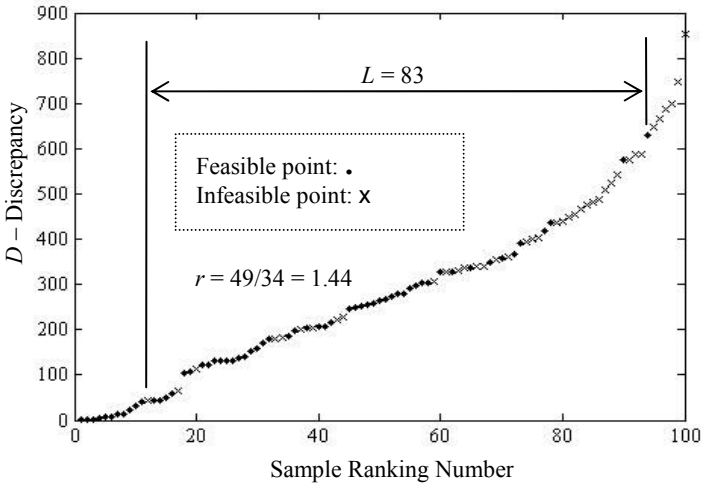

Figure 2. Distribution of *D* of 100 random sample points with 2 experiments.

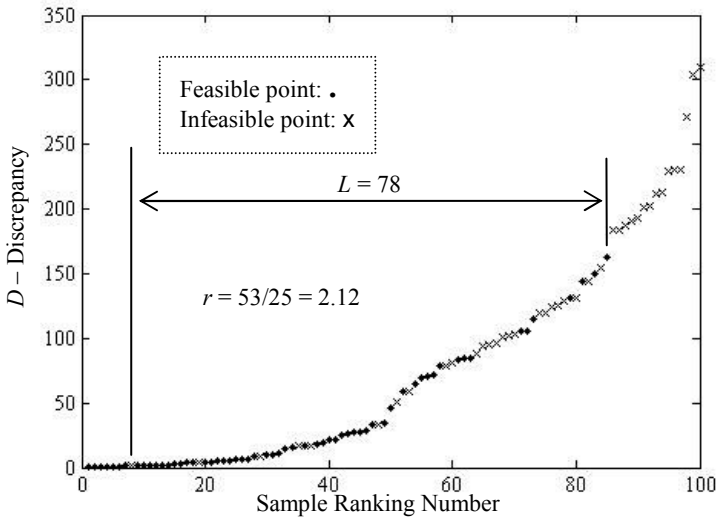

Figure 3. Distribution of *D* of 100 random sample points with 4 experiments.

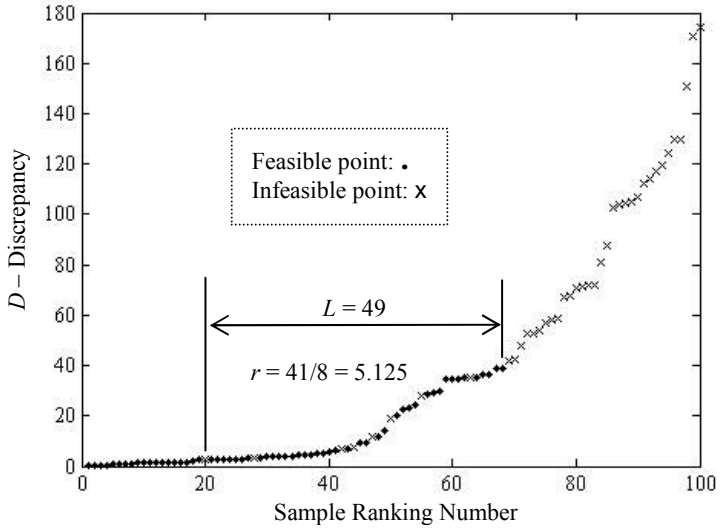

Figure 4. Distribution of *D* of 100 random sample points with 6 experiments.

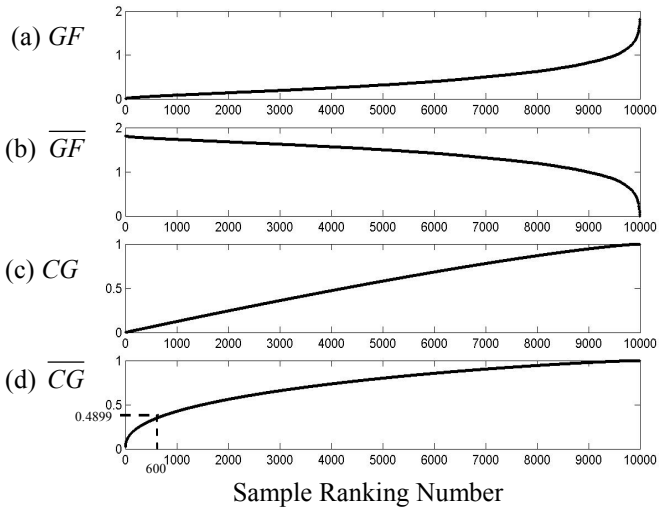

Figure 5. Construction of the Sampling Guidance Function.

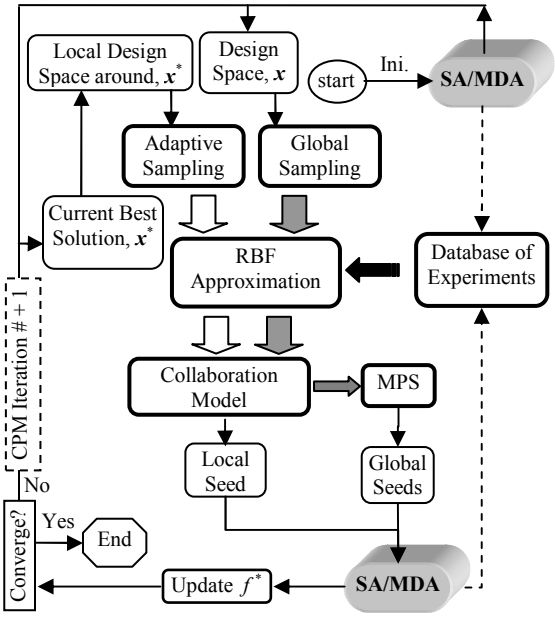

Figure 6. Architecture of the Collaboration Pursuing Method.

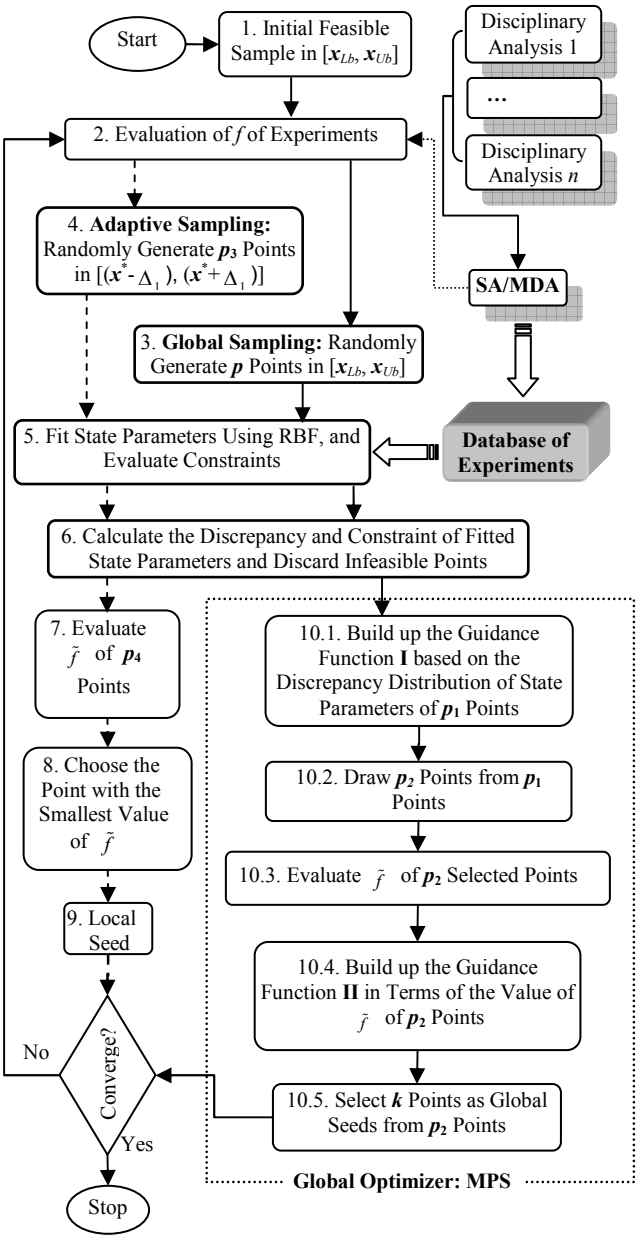

Figure 7. Flowchart of the Collaboration Pursuing Method.

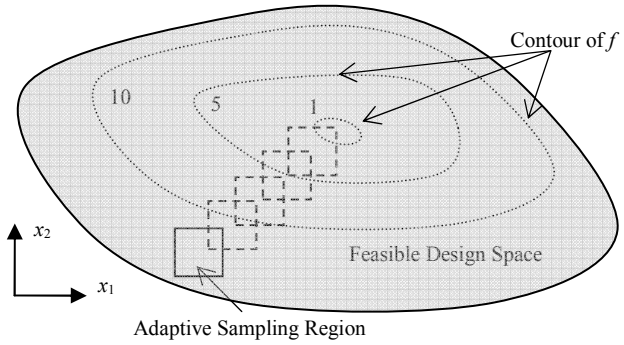

Figure 8. Description of the Adaptive Sampling for a minimization problem.

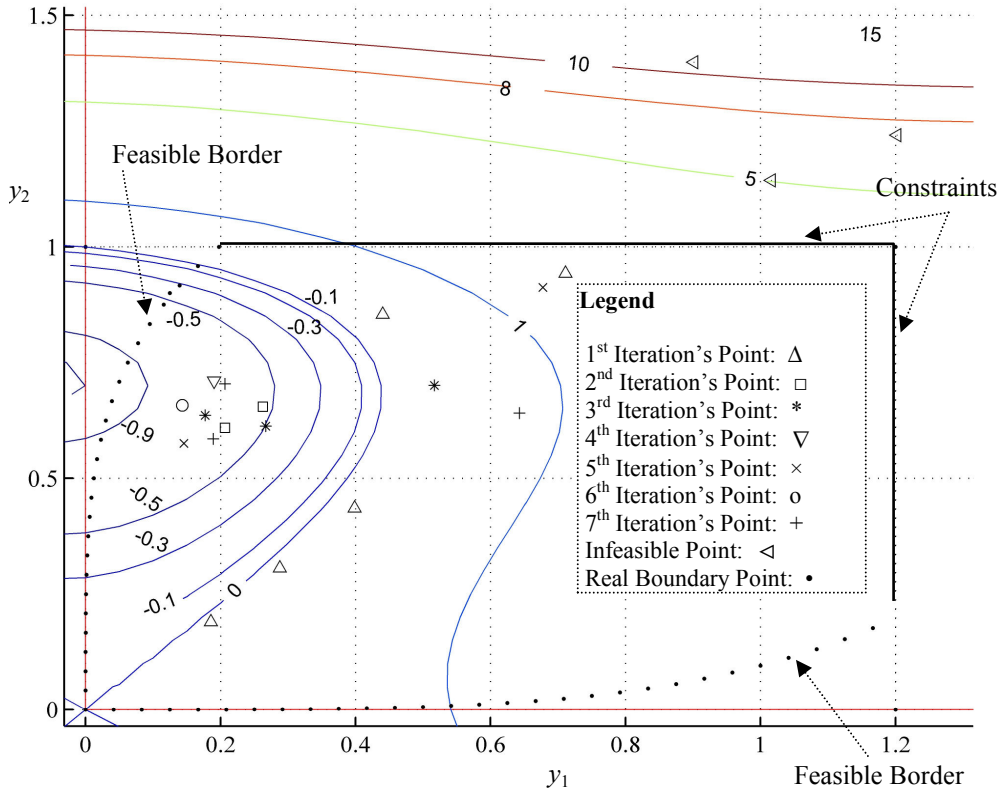

Figure 9. The optimization process of Test Case 1 solved with CPM.

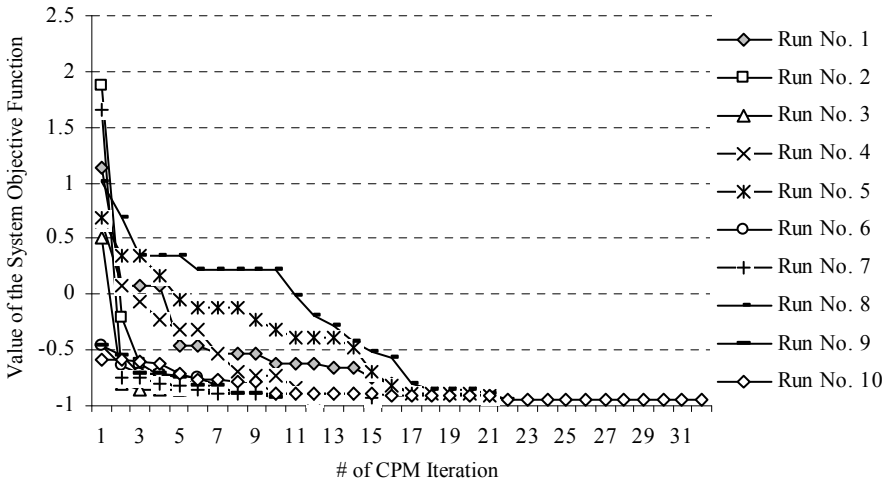

Figure 10. Intermediate best objective function values over 32 CPM iterations of Runs No. 1 – 10 in Test Case 1.

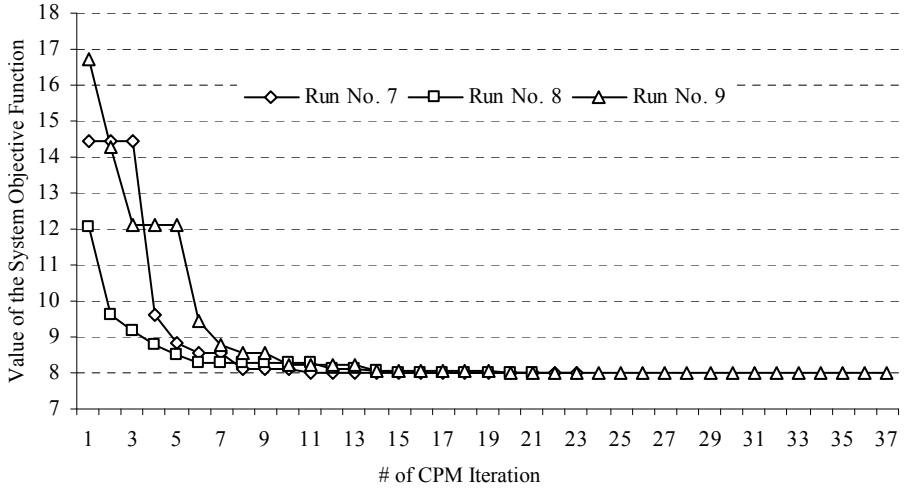

Figure 11. Intermediate best objective function values over 37 CPM iterations of Runs No. 7 – 9 in Test Case 2.

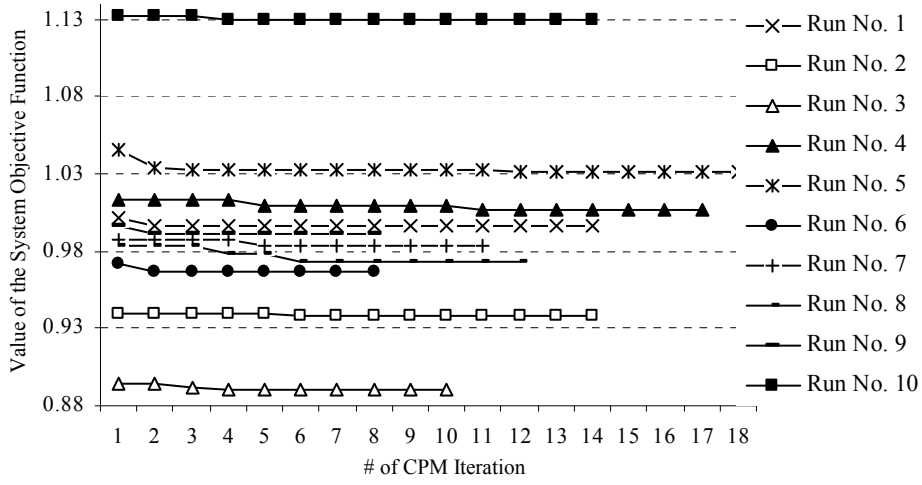

Figure 12. Intermediate best objective function values over 12 CPM iterations of Runs No. 1 – 10 in Test Case 3.

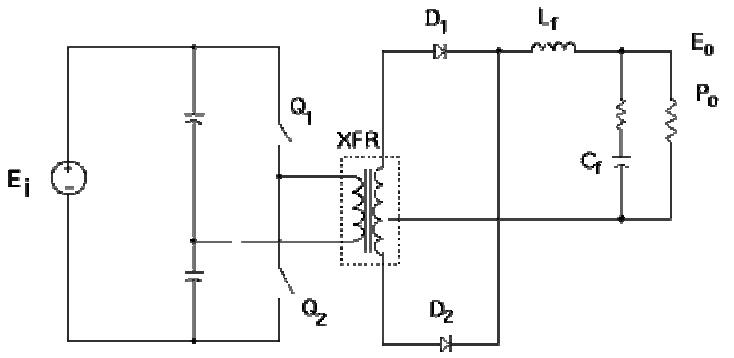

Figure 13. A schematic of the power stage of the power converter.[37]

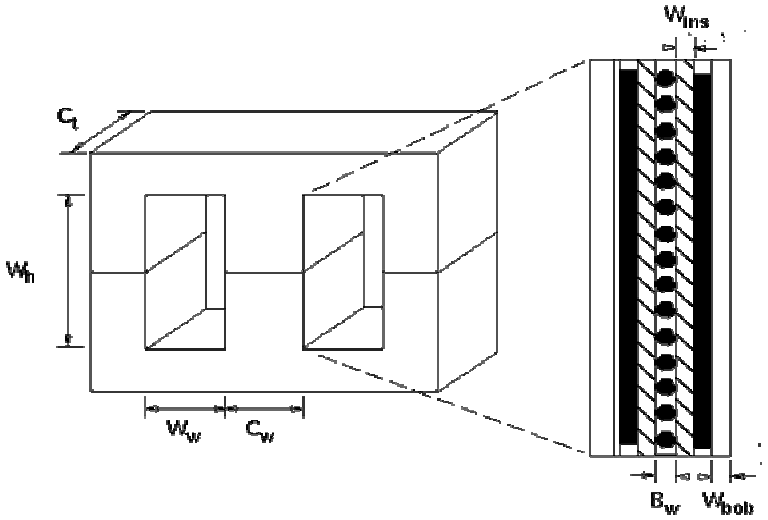

Figure 14. Geometry of the transformer core.[37]

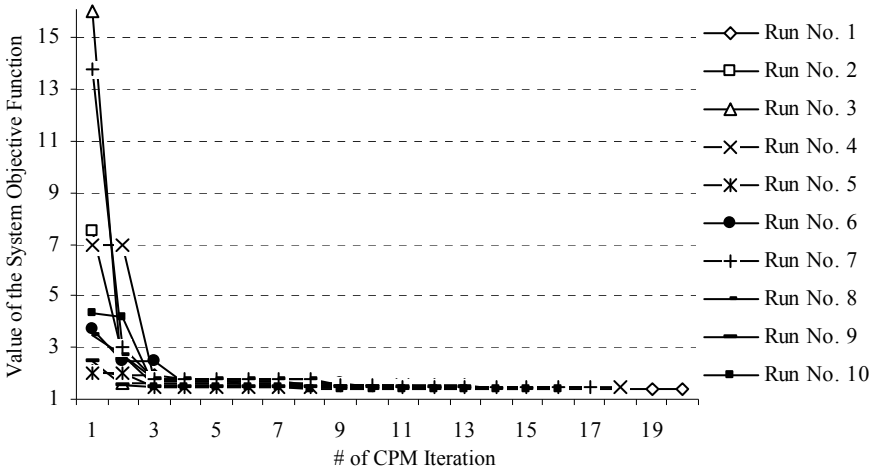

Figure 15. Intermediate best objective function values over 18 CPM iterations of Runs No. 1 – 10 in Test Case 4.

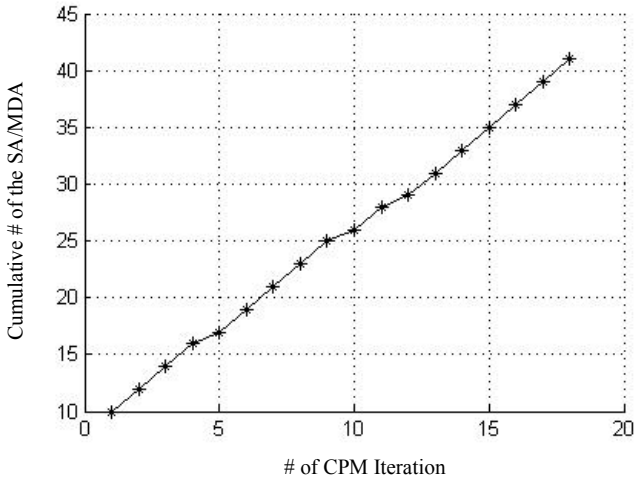

Figure 16. Cumulative number of the SA/MDA processes over 18 CPM iterations of Run No. 4 in Test Case 4.